Ground-state cooling of a mechanical oscillator and detection of a weak force using a Bose-Einstein condensate

Sonam Mahajan,[1] Tarun Kumar,[1] Aranya B. Bhattacherjee,[2] and ManMohan[1]
[1]*Department of Physics and Astrophysics, University of Delhi, Delhi 110007, India*
[2]*Department of Physics, ARSD College, University of Delhi (South Campus), New Delhi 110021, India*
(Received 8 September 2012; published 18 January 2013)

We investigate the possibility of cooling a mechanical oscillator to its ground state and using it to detect a weak coherent force by means of a hybrid optomechanical quantum device formed by a Bose-Einstein condensate (BEC) confined in a high quality factor optical cavity with an oscillatory end mirror. We show using the stochastic cooling technique that the atomic two-body interaction can be utilized to cool the mirror and achieve position squeezing essential for making sensitive measurements of weak forces. We further show that for certain values of the system parameters and spectral range, the atomic two-body interaction can also increase the signal-to-noise ratio and decrease the noise of the off-resonant stationary spectral measurements. We show that the minimum noise is obtained only in the presence of BEC.

DOI: 10.1103/PhysRevA.87.013621 PACS number(s): 03.75.Kk, 03.75.Lm, 42.50.Lc, 03.65.Ta

I. INTRODUCTION

Recently, optomechanics has been the subject of extensive theoretical and experimental investigations. The interaction between a movable mirror and the radiation field of an optical cavity provides a sensitive device which is able to detect weak forces. Significant examples of research in this area are the gravitational wave detection interferometers [1,2] and atomic force microscopes [3,4]. Over the past years, the field of laser cooling [5–7] and gravitational wave detectors [1,2] have used the interaction of mechanical and optical degrees of freedom via radiation pressure. In recent years, the interest has emerged in the application of radiation force to change the center-of-mass motion of mechanical oscillators, covering a vast range of scales from macroscopic mirrors in the Laser Interferometer Gravitational Wave Observatory (LIGO) project [8] to nanomechanical cantilevers [9–14], vibrating micro-toroids [15,16], and membranes [17]. Detection of weak forces using a cantilever is of much interest in many applications such as magnetometry of nanoscale magnetic particles [18], femtojoule calorimetry [19], and other numerous types of force microscopy [20]. A measured force resolution of 5.6×10^{-18} N/$\sqrt{\text{Hz}}$ at 4.8 K in vacuum using cantilever-based technology has been demonstrated [21].

The detection of displacement with high sensitivity is possible due to the capability of optical interferometry which has been shown recently in optical interferometry experiments [22,23] and advances in gravitational wave detectors [24]. Experimentally, highly sensitive optical displacement measurements can be done using a sensor which shows a direct effect of radiation pressure, back action effect, that every optical experiment will be sensitive to if quantum noise is limited [11]. The possibility of gravitational wave detection using atom field interferometers has been reported recently [25]. Much new possibility arises in cavity optomechanics when the experimental and theoretical tools of cavity quantum electrodynamics (QED) are combined with those of ultracold gases [26–38]. If a collection of atoms is placed in a high-finesse optical cavity then the atoms collectively interact with the light mode thereby increasing the atom-field interaction. The coupling of the coherent motion of the condensate atoms trapped in an optical lattice, formed by a high-finesse optical cavity and the intracavity field, give rise to nonlinear quantum optics [29]. Even if the average photon number is as small as 0.05, one can observe strong optical nonlinearities [29]. Earlier experiments have shown important progress in the field of cavity QED by combining it with ultracold atoms [39–41].

Thermal noise, which arises due to the mechanical motion of the mirror, is the major hurdle in achieving the sensitive optical measurements [23,42]. It can be reduced using various feedback schemes based on the homodyne detection of the reflected light of the oscillator [43]. A continuous version of the stochastic cooling feedback technique, used in accelerators [44], helps in cooling the mirror of the optomechanical system as the feedback regularly "kicks" the mirror from the back and the position is regularly monitored using homodyne detection. In the presence of the feedback, it is important to describe the whole system quantum mechanically for two reasons. First it permits developing a condition for optomechanical systems under which the effects of quantum noise becomes visible and experimentally detectable. Lastly it establishes the ultimate limits of the proposed feedback scheme. Stochastic cooling feedback is one of the effective techniques used to cool optomechanical devices. It can provide efficient cooling as shown in recent experiments [12,45,46]. It has several advantages over other feedback techniques as suggested [43]. This feedback scheme reduces the thermal noise of the device even for small frequencies, i.e., out of resonance. Also this technique can beat the standard quantum limit in certain conditions. Moreover, it can also be used to generate stationary contractive states [47].

A hybrid optomechanical system consisting of Bose-Einstein condensate (BEC) in an optical cavity with vibrating end mirror has been studied [48]. This study revealed that the hybrid system was useful for accomplishing state engineering of the vibrational mode of the mechanical oscillator by virtue of coupling to the BEC, which is less sensitive to noise effects and more easily controlled. Given the necessity to improve the signal-to-noise ratio or sensitivity of position measurements especially for gravitational wave detection [1,2] or for

metrological applications [49] and promising developments in the field of ultracold atoms and cavity optomechanics, we propose in this paper a scheme to couple a Bose-Einstein condensate to an optical cavity with a movable mirror to detect weak forces using the stochastic cooling scheme. Apart from the robust nature of the BEC and the many advantages of stochastic cooling technique as noted above, we propose to utilize the atomic two-body interaction (tunable using Feshbach resonance technique) to coherently detect weak forces. The addition of the BEC acts as an additional sink at extremely low temperature, which can extract energy from the moving mirror, thereby making the system more sensitive to external noise. From the experimental side, coupling between an oscillating membrane and ultracold atoms mediated by cavity photons has been demonstrated recently [50].

II. THE BASIC MODEL

The system investigated here consists of a coherently driven Fabry-Perot cavity with one mirror fixed and the second mirror movable (Fig. 1). This basic optomechanical setup is the basis of detecting weak forces in gravitational wave detectors [1,2] and atomic force microscopy [3,4]. In our model, we have in addition an elongated cigar-shaped gas of N two-level ultracold atoms of ^{87}Rb in the $|F=1\rangle$ state having mass m and transition frequency ω_a of the $|F=1\rangle \rightarrow |F'=2\rangle$ transition of the D_2 line. The cloud of BEC is interacting with a single quantized mode of the cavity with frequency ω_c. The cavity mode is also forming an optical lattice potential between the two mirrors. The sensitivity of the proposed quantum device to measure weak forces (shown in Fig. 1) is eventually determined by the quantum fluctuations. In order to minimize the quantum fluctuations associated with the various modes of the vibrating mirror, we consider the mirror as a single quantum-mechanical harmonic oscillator with frequency ω_m and mass M_m. Experimentally this approximation can be realized [51] if we use a bandpass filter in the detection loop,

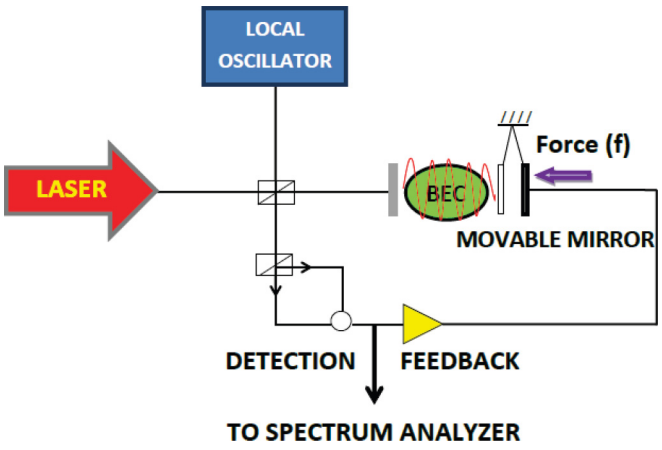

FIG. 1. (Color online) Schematic representation of the setup. Figure shows an optomechanical system with Bose-Einstein condensate (BEC) confined in an optical cavity with one mirror fixed and other moving. Here the cavity mode is driven by the laser, which also provides the local oscillator for the homodyne measurement using the beam splitter. The external force (f) to be measured acts on the movable mirror.

so that the frequencies are limited to a narrow bandwidth which includes a single mechanical resonance. An external pump with frequency ω_p is also incident from the fixed mirror, which is a constant source of photons for the cavity. Intracavity photons exert pressure on the mirrors and this results in an optomechanical coupling between the cavity field and the movable mirror. The cavity light field exerts a force on the movable mirror which depends on the intracavity photons. The light in turn is phase shifted by an amount $2\kappa l_m$, where κ is the wave vector and l_m is the displacement of the mirror from its equilibrium position. In the adiabatic limit i.e., $\omega_m \ll c/2L$ (L is the length of the optical cavity), single-mode approximation of the cavity field is valid since photon scattering into other modes can be ignored. This system can be described by an optomechanical Hamiltonian in rotating wave and dipole approximation as [26]

$$\begin{aligned} H &= E_0 \sum_j b_j^\dagger b_j + J_0(\hbar U_0 a^\dagger a + V_{cl}) \sum_j b_j^\dagger b_j \\ &+ \frac{U}{2} \sum_j b_j^\dagger b_j^\dagger b_j b_j - \hbar \Delta_c a^\dagger a - i\hbar\eta(a - a^\dagger) \\ &+ \hbar\omega_m a_m^\dagger a_m - \hbar\epsilon\omega_m a^\dagger a(a_m + a_m^\dagger), \end{aligned} \tag{1}$$

where

$$\begin{aligned} U &= \frac{4\pi a_s \hbar^2}{m} \int d^3x |w(\vec{r})|^4, \\ E_0 &= \int d^3x w(\vec{r} - \vec{r}_j) \left\{ \left(-\frac{\hbar^2 \nabla^2}{2m} \right) \right\} w(\vec{r} - \vec{r}_j), \\ J_0 &= \int d^3x w(\vec{r} - \vec{r}_j) \cos^2(kx) w(\vec{r} - \vec{r}_j). \end{aligned} \tag{2}$$

Here b_j, a, and a_m are the condensate annihilation operators at the jth site, cavity mode annihilation operator, and mirror mode (phonon) annihilation operator, respectively. $\Delta_c = \omega_p - \omega_c$ is the cavity pump detuning. Here η is the strength of the external pump. The mirror-photon coupling is $G = \epsilon\omega_m$ and V_{cl} is the external classical potential. $U_0 = g_0^2/\Delta_a$ is the optical lattice barrier height per photon where g_0 is the atom-photon coupling and $\Delta_a = \omega_p - \omega_a$ is the atom-pump detuning. We shall consider from now on $U_0 > 0$. In this case the condensate atoms are pulled towards nodes of the cavity light field and as a result the lowest bound state is localized at the nodes. This leads to a reduced coupling of the condensate atoms to the cavity field compared to that for $U_0 < 0$. Also E_0 and J_0 are the effective on-site energies of the condensate defined in terms of the condensate atomic Wannier function $w(\vec{r} - \vec{r}_j)$. U is the effective on-site atom-atom interaction energy, where a_s is the s-wave scattering length. In deriving the above Hamiltonian Eq. (1), we have ignored the tunneling of atoms into neighboring wells. We can experimentally achieve this by tuning the optical lattice depth so that time scales over which tunneling takes place is much larger than the times scales over which the experiment is performed. The cavity mode formed by the input pump laser couples to the mechanical oscillator (movable mirror) through radiation pressure and the condensate atoms through the dipole interaction. The back-action of the atoms and cantilever modifies the cavity field. The nonlinearity in Eq. (1) arising from the coupling

between the intracavity intensity and the position quadrature of the cantilever plays a significant role in the system dynamics. The system we are considering is basically an open system since the cavity field is damped due to the leakage of the photons through the cavity mirrors. Moreover the cantilever is connected to a bath at finite temperature (T). The mechanical oscillator is expected to undergo a pure Brownian motion driven by its contact with the thermal environment in the absence of any radiation pressure due to the cavity light field. Let us now understand the origin of each of the terms appearing in the Hamiltonian of Eq. (1). The first term is simply the on-site kinetic energy of the condensate. The second term is the coupling of the condensate with the cavity field which also includes the classical potential V_{cl}. The third term is the two-body atom-atom interaction term. The fourth term is the photon energy, and the fifth term corresponds to the pump. The sixth term is the energy of the single mode of the mirror, and the seventh term is the energy associated with the dispersive nonlinear coupling between the cavity field and the mirror.

Dissipation enters the system through its interaction with the external degrees of freedom. The cavity optical field is damped (decay constant γ_c) due to the leakage of photons through the mirrors. The mirrors couple the internal cavity modes with the external electromagnetic modes. The movable mirror is damped (decay constant γ_m) due to its interaction with the external modes. The condensate is more robust and there is no significant loss of atoms during the experimental time. The dynamics of the system can be described by the following set of coupled quantum Langevin equations (QLE):

$$\begin{aligned}\dot{a}(t) = &-i J_0 U_0 a(t) \sum_j b_j^\dagger(t) b_j(t) + i\Delta_c a(t) \\ &+ i\epsilon\omega_m a(t)[a_m(t) + a_m^\dagger(t)] \\ &+ \eta - \frac{\gamma_c}{2} a(t) + \sqrt{\gamma_c} a_{in}(t), \end{aligned} \tag{3}$$

$$\begin{aligned}\dot{b_j}(t) = &-i\frac{E_0}{\hbar} b_j(t) - i\frac{J_0}{\hbar}[\hbar U_0 a^\dagger(t) a(t) \\ &+ V_{cl}] b_j(t) - i\frac{U}{\hbar} b_j^\dagger(t) b_j(t) b_j(t), \end{aligned} \tag{4}$$

$$\dot{a}_m(t) = -i\omega_m a_m(t) + i\epsilon\omega_m a^\dagger(t) a(t) - \gamma_m a_m(t) + \sqrt{\gamma_m}\xi_m(t), \tag{5}$$

where $a_{in}(t)$ and $\xi_m(t)$ are the input noise operators for the cavity field and mirror, respectively, with the correlations [52] defined in Appendix A.

The steady-state cavity field (β) can be derived from Eqs. (3), (4), and (5) in terms of the steady-state value of the phonon operator α and the number of atoms N by putting the time derivative to zero:

$$\beta = \frac{\eta}{-i\Delta_c + \frac{\gamma_c}{2} + i J_0 U_0 N - i 2\mathrm{Re}(\alpha)\epsilon\omega_m}, \tag{6}$$

$$\mathrm{Re}(\alpha) = \frac{\epsilon\omega_m^2 |\beta|^2}{\omega_m^2 + \gamma_m^2}. \tag{7}$$

One can identify from the above equations that the steady state of the cavity field is influenced by the dynamics of the mirror and the atoms. The resonance frequency of the cavity is shifted due to its interaction with the mirror and the atoms in such a way so as to form a new stationary intensity. After a transient time, the cavity field changes depending on the response of the field and the strength of the interaction with the condensate and the mirror.

We are now interested in the dynamics of fluctuations around the steady state. To this end, we linearize the QLE [Eqs. (3), (4), and (5)] around the steady state as $a(t) \to \beta + a(t)$, $a_m(t) \to \alpha + a_m(t)$, and $b_j(t) \to \frac{\sqrt{N}+b(t)}{\sqrt{M}}$. Here β, α, and $\sqrt{N/M}$ are the steady state of the photon, phonon, and the atomic fields, respectively. M is the total number of lattice sites occupied by N atoms. We also replace $b_j(t)$ by $b(t)$, assuming that all the sites of the optical lattice are identical. Consequently, we get

$$\begin{aligned}\dot{a}(t) = &\left[i\Delta_d - \frac{\gamma_c}{2}\right] a(t) - i g_c [b(t) + b^\dagger(t)] \\ &+ iG\beta[a_m(t) + a_m^\dagger(t)] + \sqrt{\gamma_c} a_{in}(t), \end{aligned} \tag{8}$$

$$\begin{aligned}\dot{b}(t) = &-i[\nu + 2U_{\mathrm{eff}}] b(t) - i U_{\mathrm{eff}} b^\dagger(t) \\ &- i g_c [a(t) + a^\dagger(t)], \end{aligned} \tag{9}$$

$$\begin{aligned}\dot{a}_m(t) = &-i\omega_m a_m(t) + iG\beta[a(t) + a^\dagger(t)] \\ &- \gamma_m a_m(t) + \sqrt{\gamma_m}\xi_m(t), \end{aligned} \tag{10}$$

where $\Delta_d = -J_0 U_0 N + \Delta_c + 2G\alpha$, $g_c = J_0 U_0 \beta\sqrt{N}$, $G = \epsilon\omega_m$, $\nu = E_0/\hbar + J_0 U_0 \beta^2 + J_0 V_{cl}/\hbar$, and $U_{\mathrm{eff}} = UN/\hbar M$. In the following, we will always take $\Delta_d = 0$, relevant to many experimental situations.

We now introduce the following amplitude and phase quadratures: $X(t) = [a(t) + a^\dagger(t)]$, $Y(t) = i[a^\dagger(t) - a(t)]$, $Q(t) = [a_m(t) + a_m^\dagger(t)]$, $P(t) = i[a_m^\dagger(t) - a_m(t)]$, $Q_c(t) = [b(t) + b^\dagger(t)]$, $P_c(t) = i[b^\dagger(t) - b(t)]$, $X_{in}(t) = [a_{in}(t) + a_{in}^\dagger(t)]$, $Y_{in}(t) = i[a_{in}^\dagger(t) - a_{in}(t)]$.

$$\dot{X}(t) = -\frac{\gamma_c}{2} X(t) + \sqrt{\gamma_c} X_{in}(t), \tag{11}$$

$$\dot{Y}(t) = -\frac{\gamma_c}{2} Y(t) - 2g_c Q_c(t) + 2G\beta Q(t) + \sqrt{\gamma_c} Y_{in}(t), \tag{12}$$

$$\dot{Q}_c(t) = (\nu + U_{\mathrm{eff}}) P_c(t), \tag{13}$$

$$\dot{P}_c(t) = -(\nu + 3U_{\mathrm{eff}}) Q_c(t) - 2g_c X(t), \tag{14}$$

$$\dot{Q}(t) = \omega_m P(t), \tag{15}$$

$$\dot{P}(t) = -\omega_m Q(t) + 2G\beta X(t) - \gamma_m P(t) + W(t), \tag{16}$$

where $W(t) = i\sqrt{\gamma_m}[\xi_m^\dagger(t) - \xi_m(t)]$, which satisfies the correlation given in Appendix A. From the above Eqs. (11)–(16), we observe that the phase quadrature of the cavity is only affected by the mirror position fluctuations $Q(t)$ and the condensate position fluctuations $Q_c(t)$. In general, we notice that it is only the phase quadratures which are affected by the fluctuations.

III. FEEDBACK IN STOCHASTIC COOLING SCHEME

In most applications the mechanical oscillator (movable mirror) is used as a quantum meter to detect weak forces

acting on it [53]. Consequently, the term that describes the action of the classical external force $f(t)$ on the mirror position $(a_m + a_m^\dagger)$ is given as

$$H_f = -\frac{\hbar}{2}(a_m + a_m^\dagger) f(t). \tag{17}$$

The force to be measured appears in the phase quadrature of the mirror only:

$$\dot{P}(t) = -\omega_m Q(t) + 2G\beta X(t) + f(t) - \gamma_m P(t) + W(t). \tag{18}$$

Such a force can be measured by looking at the mirror's position quadrature $Q(t)$. In the large cavity bandwidth limit, i.e., $\gamma_c \gg G\beta, \omega_m$, the cavity mode dynamics adiabatically follows that of the movable mirror. Therefore,

$$X(t) = \frac{2}{\sqrt{\gamma_c}} X_{in}(t), \tag{19}$$

$$Y(t) = -\frac{4g_c}{\gamma_c} Q_c(t) + \frac{4G\beta}{\gamma_c} Q(t) + \frac{2}{\sqrt{\gamma_c}} Y_{in}(t). \tag{20}$$

In the large cavity bandwidth limit, the weak force can be measured by monitoring the dynamics of the mirror position $Q(t)$, through the homodyne measurement of the phase quadrature $Y(t)$. Homodyne detection is a method of detecting frequency-modulated radiation by nonlinear mixing with radiation of a reference frequency (local oscillator). In homodyne detection, the reference frequency equals that of the input signal radiation. The dynamics of the cantilever can be controlled through a phase sensitive feedback loop which may be devised using the output of a homodyne measurement. Interestingly, the phase quadrature $Y(t)$ now also depends on the position of the condensate $Q_c(t)$. It should then be possible to control $Y(t)$ through condensate parameters ν and $U_{\rm eff}$. The experimentally detected quantity is the output homodyne photocurrent [43],

$$Y_{\rm out} = 2\eta' \sqrt{\gamma_c} Y(t) - \sqrt{\eta'} Y_{in}^{\eta'}(t), \tag{21}$$

where η' is the detector efficiency, $Y_{in}^{\eta'}(t)$ is a generalized phase input noise, and $a_{\eta'}(t)$ is the generalized input noise, which satisfies the correlations given in Appendix A. In the stochastic cooling scheme, the homodyne measurement provides a continuous monitoring of the oscillator's position and the feedback continuously kicks the mirror to put it back in its equilibrium position. When photons exert radiation pressure on the mirror in the cavity, it displaces the mirror from its equilibrium position. To bring back the mirror to equilibrium position, a pressure is exerted on the mirror from opposite side through feedback. This helps in cooling down the mirror. This technique uses the phase-sensitive noise to cool the mirror. The feedback loop consists of a transducer which converts the random optical signal to a stochastic electric signal which in turn mechanically drives the mirror's momentum. This results in an additional term in the QLE for any generic operator $A(t)$ given by [43],

$$\dot{A}_{fb}(t) = \frac{i\sqrt{\gamma_c}}{\eta'} Y_{\rm out}(t-\tau)[g_{sc} P(t), A(t)], \tag{22}$$

where τ is the feedback loop delay time and g_{sc} is a dimensionless feedback gain factor. In the limit of zero delay time $\tau \to 0$, we have the only nonzero dynamics of the feedback operator,

$$\dot{Q}_{fb} = \frac{\sqrt{\gamma_c}}{\eta'} g_{sc} Y_{\rm out}(t). \tag{23}$$

As a result, the QLE for $Q(t)$ is modified as

$$\dot{Q}(t) = \omega_m P(t) - 8 g_{sc} g_c Q_c(t) + 8G\beta g_{sc} Q(t) + 4\sqrt{\gamma_c} g_{sc} Y_{in}(t) - \sqrt{\frac{\gamma_c}{\eta'}} g_{sc} Y_{in}^{\eta'}(t). \tag{24}$$

The influence of the condensate on the mirror dynamics now appears due to the feedback loop.

IV. STATIONARY OSCILLATOR ENERGY

We now study the energy of the stationary state of the movable mirror, which is obtained in the $t \to \infty$ limit. We will particularly see how the two-body interactions $U_{\rm eff}$ can be used to minimize the energy. The solutions of the QLE are generally obtained by Laplace transform numerically using MATHEMATICA 8.0. Hence we obtain

$$\begin{aligned} Q(t) = {} & C_1(t) Q(0) + C_2(t) P(0) + C_3(t) Q_c(0) + C_4(t) P_c(0) \\ & + \int_0^\infty C_5(t') X_{in}(t-t') dt' \\ & + 4\sqrt{\gamma_c} g_{sc} \int_0^\infty C_1(t') Y_{in}(t-t') dt' \\ & - g_{sc} \sqrt{\frac{\gamma_c}{\eta'}} \int_0^\infty C_1(t') Y_{in}^{\eta'}(t-t') dt' \\ & + \int_0^\infty [f(t-t') + W(t-t')] C_2(t') dt'. \end{aligned} \tag{25}$$

Similarly,

$$\begin{aligned} P(t) = {} & -\omega_m C_6(t) Q(0) + C_7(t) P(0) + C_8(t) Q_c(0) \\ & + C_9(t) P_c(0) + \int_0^\infty dt' C_{10}(t') X_{in}(t-t') \\ & - 4\omega_m \sqrt{\gamma_c} g_{sc} \int_0^\infty C_6(t') Y_{in}(t-t') dt' \\ & + \omega_m \sqrt{\frac{\gamma_c}{\eta'}} g_{sc} \int_0^\infty C_6(t') Y_{in}^{\eta'}(t-t') dt' \\ & + \int_0^\infty C_7(t') [f(t-t') + W(t-t')] dt'. \end{aligned} \tag{26}$$

Now using the correlations of noise as given in Appendix A, we find the stationary values of $\langle Q^2 \rangle$ and $\langle P^2 \rangle$,

$$\begin{aligned} \langle Q^2 \rangle = {} & g_{sc}^2 \left(8\gamma_c + \frac{\gamma_c}{\eta'} \right) \int_0^\infty [C_1(t)]^2 dt \\ & + \frac{\gamma_m k_B T}{\hbar \omega_m} \int_0^\infty [C_2(t)]^2 dt + \int_0^\infty [C_5(t)]^2 dt, \end{aligned} \tag{27}$$

$$\begin{aligned} \langle P^2 \rangle = {} & \omega_m^2 g_{sc}^2 \left(8\gamma_c + \frac{\gamma_c}{\eta'} \right) \int_0^\infty [C_6(t)]^2 dt \\ & + \frac{\gamma_m k_B T}{\hbar \omega_m} \int_0^\infty [C_7(t)]^2 dt + \int_0^\infty [C_{10}(t)]^2 dt. \end{aligned} \tag{28}$$

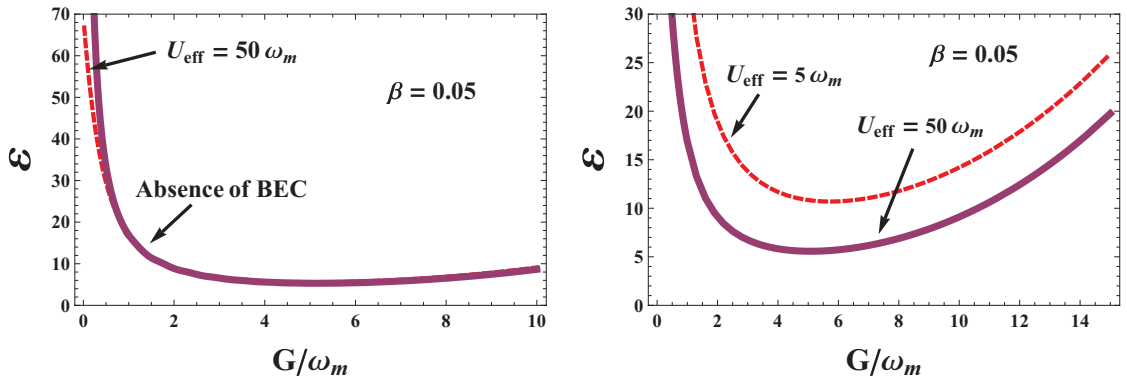

FIG. 2. (Color online) Plot of steady-state energy (dimensionless with respect to ω_m) as a function of mirror-photon coupling G/ω_m. The parameters used are $\gamma_m/\omega_m = 10^{-5}$, $\gamma_c/\omega_m = 1.5$, $g_{sc} = -0.5$, $\eta' = 0.8$, $\beta = 0.05$, $k_BT/\hbar\omega_m = 10^5$, $\nu/\omega_m = 2$, $g_c = 1.42\omega_m$. Here left-hand plot shows the variation of the steady-state energy in the absence of BEC (solid line) and in the presence of BEC (dashed line) with $U_{\rm eff}/\omega_m = 50$. Also, right-hand plot shows the variation of steady-state energy for two values of atomic two-body interaction $U_{\rm eff}/\omega_m = 5$ (dashed line) and $U_{\rm eff}/\omega_m = 50$ (solid line).

The various coefficients appearing in $Q(t)$ and $P(t)$ are given in Appendix B. The second term in the above equations for $\langle Q^2\rangle$ and $\langle P^2\rangle$ is the contribution of the quantum Brownian motion. We have used the high-temperature approximation $\coth(\hbar\omega/2k_BT) \approx 2k_BT/\hbar\omega$. The quality factor $Q_f = \omega_m/\gamma_m$ has to be high in order to reduce the affect of the thermal contribution. We now study the stationary oscillator energy $U_{st} = \frac{\hbar\omega_m}{2}[\langle Q^2\rangle + \langle P^2\rangle]$ and investigate the influence of the condensate two-body interaction $U_{\rm eff}$ and the renormalized atom-photon coupling constant g_c on the cooling of the mirror. In the figures, we will always plot the dimensionless steady-state energy $\epsilon = 2U_{st}/\hbar\omega_m$. The left plot of Fig. 2 illustrates the steady-state energy as a function of dimensionless mirror-photon coupling G in the absence of BEC (solid line) and in the presence of BEC (dashed line). Clearly we observe that the oscillator energy is reduced in the presence of BEC for small values of G. For higher values of G, the two plots merge and approached the ground state of the mirror. The right plot of Fig. 2 depicts the steady-state energy as a function of G for two values of $U_{\rm eff} = 5\omega_m$ (dashed line) and $U_{\rm eff} = 50\omega_m$ (solid line). A substantial lowering of oscillator energy is noticed for higher $U_{\rm eff}$. Variation of the steady-state oscillator energy with $U_{\rm eff}$ is shown in the left plot of Fig. 3. A rapid initial decline in the oscillator energy with increasing $U_{\rm eff}$, followed by a steady value near the ground-state value of the energy for higher $U_{\rm eff}$, is noticed.

Coupling between the condensate atoms, the cavity field and the mirror mode leads to a resonant energy exchange between the three systems. Such energy exchange leads to normal mode splitting [26]. In our earlier work [26], we had shown that the condensate atoms participate in the energy exchange only in the presence of a finite two-body interaction $U_{\rm eff}$ indicating that the Bogoliubov mode of the condensate is involved in the three-mode coupling. In a recent experiment [28], coupling of a cloud of ultracold atoms to an optical resonator suggest that the Bogoliubov modes interacting significantly with the cavity field are those with momentum $\pm 2k_c$ (k_c is the cavity wave number). The observed decrease in the energy of the mirror with increase in $U_{\rm eff}$ could be due to resonant transfer of energy from the mirror mode to the condensate mode via the cavity mode. The indirect coupling (mediated by the cavity field) to the collective excitations of the condensate determines the number of thermal excitations in the mechanical mode and hence its energy. The BEC can absorb energy taken from the mirror by the cavity field. Increase in membrane (coupled to a BEC

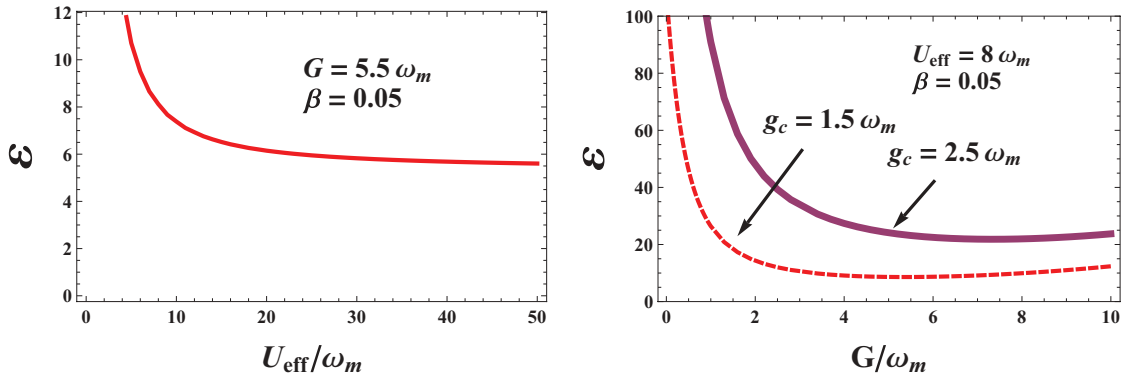

FIG. 3. (Color online) Left plot: Plot of steady-state energy as a function of $U_{\rm eff}/\omega_m$. Right plot: Plot of steady-state energy versus mirror-photon coupling G/ω_m for two values of g_c. Parameters used are same as in Fig. 2.

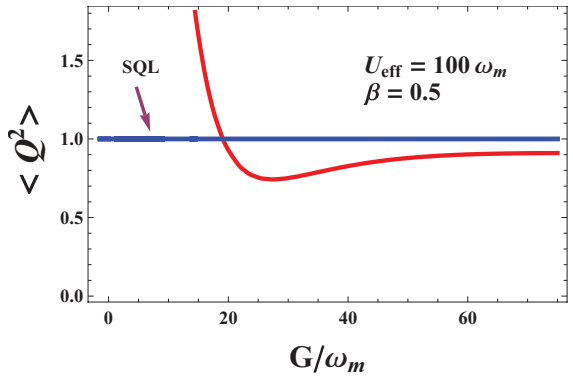

FIG. 4. (Color online) Steady-state position variance $\langle Q^2\rangle$ as a function of mirror-photon coupling G/ω_m for $\gamma_m/\omega_m = 10^{-4}$, $\gamma_c/\omega_m = 1.5$, $g_{sc} = -2.0$, $\eta' = 1.0$, $g_c = 14.23\omega_m$, $\beta = 0.5$, $k_BT/\hbar\omega_m = 10^4$, $\nu/\omega_m = 2$, $U_0/\omega_m = 0.3$, $J_0/\omega_m = 3$, and $U_{\rm eff}/\omega_m = 100$. The horizontal full (blue line) line denotes the standard quantum limit (SQL).

via cavity mode) dissipation due to increase in atom number has been demonstrated experimentally [50]. Note that $U_{\rm eff}$ is directly proportional to the atom number N. This experiment confirms our result that increase in $U_{\rm eff}$ decreases the mirror energy.

The influence of the three-mode coupling is also seen in right plot of Fig. 3 where we have plotted the steady-state energy of the oscillator as a function of G for two values of renormalized atom-photon coupling g_c. As g_c increases, the energy of the mechanical mode increases, suggesting that energy is being transferred from the condensate mode to the mirror mode via the cavity mode due to atomic back action. This observation is consistent with earlier results [48]. The above results reveal that on one hand increasing $U_{\rm eff}$ decreases the energy of the mirror, on the other hand increasing g_c increases the energy of the mirror. In order to measure any weak force acting on the mirror an optimal value of mirror energy can be achieved with the two handles, $U_{\rm eff}$ and g_c. We found that in the absence of feedback ($g_{sc} = 0$), the energy substantially increases and the BEC no longer influences the mirror motion, which can be seen from Eq. (24). In the absence of feedback only the $Y(t)$ quadrature of the cavity photons is influenced by the BEC [Eq. (12)].The influence of the BEC on the mirror position appears due to the feedback loop.

This stochastic cooling scheme can also be used to achieve steady-state position squeezing, i.e, to overcome the standard quantum limit $\langle Q^2\rangle_{st} < 1$. The possibility to beat the standard quantum limit for the oscillator position uncertainty is shown in Fig. 4, where $\langle Q^2\rangle_{st}$ is plotted as a function of G. The standard quantum limit is seen to be beaten in some specific parameter regime as found in Fig. 4. Note that while the uncertainty in the oscillator position decreases, the corresponding uncertainty in the oscillator momentum increases and as a result of which the total oscillator stationary energy $U_{st} = \frac{\hbar\omega_m}{2}[\langle Q^2\rangle + \langle P^2\rangle]$ increases. Consequently, it is not necessary that steady-state oscillator position squeezing and oscillator ground-state cooling be achieved in the same parameter range. Ground-state oscillator energy is approached for $\langle Q^2\rangle \approx \langle P^2\rangle$.

V. NOISE POWER SPECTRUM

The oscillator energy studied in the previous section ultimately has to be measured in the form of the noise power spectrum of the mirror. Here we investigate the signal-to-noise ratio (SNR) of the optomechanical device. The signal corresponding to the spectral measurement in terms of the directly measured quantity "output homodyne photocurrent" $Y_{\rm out}(t)$ is defined as [43]

$$S(\omega) = \left|\int_{-\infty}^{\infty} dt e^{-i\omega t}\langle Y_{\rm out}(t)F_{T_m}(t)\rangle\right|, \tag{29}$$

where

$$\langle Y_{\rm out}\rangle = \frac{-8\eta' g_c}{\sqrt{\gamma_c}}\langle Q_c\rangle + \frac{8\eta' G\beta}{\sqrt{\gamma_c}}\langle Q\rangle. \tag{30}$$

Here $F_{T_m}(t)$ is a filter function approximately equal to 1 in the time interval $[0, T_m]$, in which the spectral measurement is performed and equal to zero otherwise [43]. For stationary spectral measurements, the measurement time T_m is taken to be much larger than the oscillator relaxation time $1/\gamma_m$, i.e., $T_m \gg 1/\gamma_m$. In this limit, for very large measurement time T_m, one has $F_{T_m} \approx 1$. In this case, the oscillator is relaxed to equilibrium. This yields

$$S(\omega) = \frac{8\eta' G\beta}{\sqrt{\gamma_c}}|C_2(\omega) f(\omega)|, \tag{31}$$

where $f(\omega)$ is the Fourier transform of the force while $C_2(\omega)$ is the Fourier transform of $C_2(t)$. Note that the signal is independent of the BEC. The noise corresponding to the signal is given by its variance as [43]

$$N^2(\omega) = \int_{-\infty}^{\infty} dt F_{T_m}(t) \times \int_{-\infty}^{\infty} dt' F_{T_m}(t') e^{-i\omega(t-t')}\langle Y_{\rm out}(t)|Y_{\rm out}(t')\rangle_{f=0}. \tag{32}$$

Making use of the previously derived results, we arrive at the final form of the noise spectrum,

$$\begin{aligned} N^2(\omega) = {} & \frac{64\eta'^2 g_c^2}{\gamma_c} T_m |C_{11}(\omega)|^2 \\ & - \frac{128\eta'^2 G\beta g_c T_m}{\gamma_c}|C_5(\omega)C_{11}(\omega)| \\ & + \frac{64\eta'^2 G^2\beta^2}{\gamma_c} T_m \left[g_{sc}^2 \left(8\gamma_c + \frac{\gamma_c}{\eta'}\right)|C_1(\omega)|^2 \right. \\ & \left. + \frac{\gamma_m k_B T}{\hbar\omega_m}|C_2(\omega)|^2 + |C_5(\omega)|^2 \right] + 8\eta'^2 T_m + \eta' T_m \\ & + G\beta g_{sc}[128\eta'^2 + 16\eta']T_m|C_1(\omega)|, \end{aligned} \tag{33}$$

where $C_{11}(\omega)$ is Fourier transform of $C_{11}(t)$ as given in Appendix B.

The influence of the presence of BEC appears in the noise as shown in Fig. 5. As seen in Fig. 5, in the presence of BEC, the off-resonant noise decreases for $\omega > \omega_m$. Increasing $U_{\rm eff}$ would further decrease the noise significantly. In fact the minimum noise is obtained only in the presence of the BEC. At resonance $\omega = \omega_m$, the noise is practically same in the

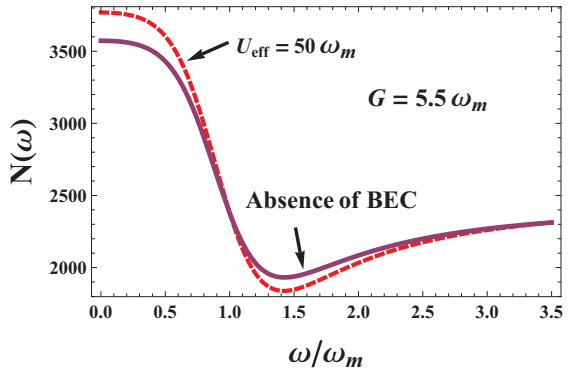

FIG. 5. (Color online) Noise spectrum as a function of ω/ω_m in the case of ideal impulsive force [$f(\omega) =$ constant]. The solid line is the plot in the absence of BEC while the dashed line is plot in presence of BEC with $U_{\rm eff}/\omega_m = 50$. The parameters used are $\gamma_m/\omega_m = 10^{-5}$, $\gamma_c/\omega_m = 1.5$, $g_{sc} = -0.5$, $\eta' = 0.8$, $\beta = 0.05$, $k_B T/\hbar\omega_m = 10^5$, $\nu/\omega_m = 2$, $g_c = 1.42\omega_m$, $f(\omega) = 10^{-5}\omega_m$, $T_m = 10^6/\omega_m$, and $G/\omega_m = 5.5$.

presence of BEC and in the absence of BEC. The top-left plot of Fig. 6 displays the SNR for two values of the atomic two-body interaction $U_{\rm eff}$ and $G/\omega_m = 0.5$. No change in the SNR is seen at resonance. The main effect of the parameter $U_{\rm eff}$ on the spectrum is the modification of the susceptibility due to the increase in the mechanical damping, which is responsible for the broadening of the spectrum. As seen above, the presence of the BEC does not influence the signal but only modifies the noise [Eq. (31)] and as a result there is no improvement in the SNR at resonance. The top-right plot of Fig. 6 shows the influence of the BEC on the noise. Interestingly increasing $U_{\rm eff}$ suppresses the off-resonant noise but not the resonant noise. The lower left plot shows the stationary signal-to-noise ratio for two values of atomic two-body interaction $U_{\rm eff}/\omega_m = 5$ (dashed line) and $U_{\rm eff}/\omega_m = 50$ (solid line) and $G/\omega_m = 5.5$ (the point where we obtain near ground state cooling). Near the ground state of the oscillator, we notice that the magnitude of the SNR is one order lower than that in the previous case ($G/\omega_m = 0.5$) and at the same time the noise is also enhanced. Interestingly, we notice that the peak SNR is suppressed for higher $U_{\rm eff}$ but overall the SNR is more for higher $U_{\rm eff}$ except for a short spectral range. For the same spectral range where the SNR is better for $U_{\rm eff}/\omega_m = 50$, the corresponding noise is lower as seen from the lower right plot. On one hand we observe that in the presence of the BEC, we are able to achieve substantial cooling of the mirror and position squeezing essential for making sensitive measurements. On the other hand, the SNR with BEC does not appear to increase the maximally available SNR. Naturally, one would always like to work where the SNR is the highest but in the present situation it would be desirable to work off resonant where the SNR in the presence of BEC is higher, so that one could take advantage of the fact that substantial cooling of the mirror is possible in the presence of the BEC. This implies

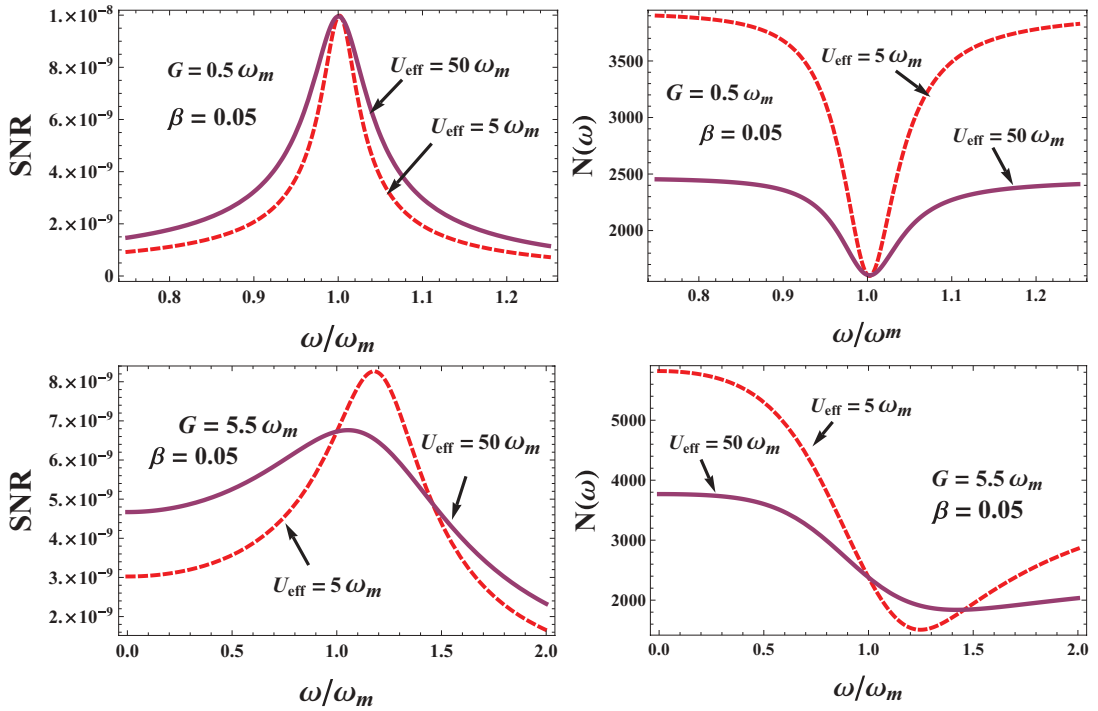

FIG. 6. (Color online) Plot of stationary signal-to-noise ratio as a function of ω/ω_m in the case of ideal impulsive force [$f(\omega) =$ constant]. The parameters used are $\gamma_m/\omega_m = 10^{-5}$, $\gamma_c/\omega_m = 1.5$, $g_{sc} = -0.5$, $\eta' = 0.8$, $\beta = 0.05$, $k_B T/\hbar\omega_m = 10^5$, $\nu/\omega_m = 2$, $g_c = 1.42\omega_m$, $f(\omega) = 10^{-5}\omega_m$, $T_m = 10^6/\omega_m$. Here top left-hand plot shows the stationary signal-to-noise ratio plot for the two values of atomic two-body interaction $U_{\rm eff}/\omega_m = 5$ (dashed line) and $U_{\rm eff}/\omega_m = 50$ (solid line) and $G/\omega_m = 0.5$. The top-right plot shows the noise spectrum for the same parameters as for the top-left plot. The lower left plot shows the stationary signal-to-noise ratio for two values of atomic two-body interaction $U_{\rm eff}/\omega_m = 5$ (dashed line) and $U_{\rm eff}/\omega_m = 50$ (solid line) and $G/\omega_m = 5.5$. The lower right plot shows the noise spectrum for the same parameters as for the lower left plot.

that an off-resonant measurement would be suitable for the measurement of the weak force acting on the mirror and for designing strategies of state engineering of the mechanical oscillator. Other schemes such as nonstationary measurements could be also suitable [54]. The two-body atomic interaction can be easily tuned using the technique of Feshbach resonance. This kind of optomechanical interactions yield a quantum interface between ultracold atoms, optical cavity mode, and mechanical mode.

In our calculations, all parameters, namely γ_c, γ_m, g_0, $U_{\rm eff}$, ω_m, and ν, are accessible in current experiments as we discuss in the following. For a BEC containing an order of 10^6 ^{87}Rb atoms [50], interacting with light field of an optical ultrahigh-finesse Fabry-Perot cavity, the strength of the coherent coupling is $g_0 = 2\pi \times 5.86$ kHz [55] ($2\pi \times 14.4$ MHz [29]) and the decay rate of the intracavity field is $\gamma_c = 2\pi \times 8.75$ kHz [55] ($2\pi \times 0.66$ MHz [29]). The contribution of the kinetic and potential energy is about $\nu = 35$ kHz [28] ($\nu = 49$ kHz [29]). Also the coherent amplification or the damping of atomic motion is neglected as the temperature (T_c) of the condensate gas $T_c \ll \hbar\gamma_c/k_B$. The atom pump detuning is $2\pi \times 32$ GHz. The scattering length of the condensate can vary from $10a_0$ to $190a_0$ (a_0 = Bohr radius) [56]. The radii of the condensate cloud can be 3.3 μm [28] (290 nm [32]) with length 20 μm [28] (615.5 nm [32]). The mechanical frequency of the resonator can vary from $2\pi \times 100$ Hz [57], $2\pi \times 10$ kHz [32], to $2\pi \times 73.5$ MHz [58]. The corresponding damping rate of the resonator thus can vary from $2\pi \times 10^{-3}$ Hz [57], $2\pi \times 3.22$ Hz [32], to $2\pi \times 1.3$ kHz [58]. The coupling rate is $G = 2\pi \times 2$ MHz. The atom field coupling is reduced as there is decrease in the energy of the cavity mode due to the loss of photons through the cavity mirrors. By using high quality factor cavities, this loss of photons can be minimized. For the perfect homodyne detection, the detector efficiency is $\eta' = 1$ and if the additional noise is taken into account then due to the inefficient detection, i.e., for the general case, $\eta' < 1$ [54]. Also in typical optomechanical experiments [23,42,59,60], the limit $\gamma_m \ll \omega_m \ll k_B T/\hbar$ is always taken.

VI. CONCLUSIONS

In conclusion we have studied how stochastic cooling scheme together with a gas of ultracold atoms confined in an optical cavity with a movable end mirror can coherently control the sensitivity of this hybrid optomechanical device. We have seen that the atom-atom two-body interaction can effectively control the cooling process of the mechanical mirror and also achieve steady-state position squeezing by beating the standard quantum limit. The atom-photon interaction on the other hand heats up the mirror. The feedback loop with the condensate appears as a new tunable handle to control the mirror dynamics. We have also analyzed the sensitivity (SNR) of the optomechanical quantum device for the case of stationary position spectral measurements for the detection of weak forces. It is found that in the presence of the BEC, the off-resonant noise decreases. We found that the presence of the condensate does not change the SNR at resonance. However if we increase the atomic two-body interaction, the off-resonant SNR is enhanced and the corresponding noise is suppressed for a certain spectral range. The system presented here appears as an optomechanical quantum device to measure weak forces by a proper choice of system parameters and spectral range. A coherent control of this device can be achieved through the two-body atom-atom interaction which can be manipulated either by the number of atoms or the s-wave scattering length.

ACKNOWLEDGMENTS

A.B. acknowledges financial support from the Department of Science and Technology, New Delhi, for financial assistance via Grant SR/S2/LOP-0034/2010. S.M. acknowledges University of Delhi for the University Teaching Assistantship.

APPENDIX A

The input noise operators for the cavity field satisfy the following correlations [43,52,54]:

$$\langle a_{in}(t)a_{in}(t')\rangle = \langle a_{in}^{\dagger}(t)a_{in}(t')\rangle = 0, \tag{A1}$$

$$\langle a_{in}(t)a_{in}^{\dagger}(t')\rangle = \delta(t-t'). \tag{A2}$$

The Brownian noise operator, $W(t) = i\sqrt{\gamma_m}[\xi_m^{\dagger}(t) - \xi_m(t)]$, satisfies the following correlation [54]:

$$\langle W(t)W(t')\rangle = \frac{1}{2\pi}\frac{\gamma_m}{\omega_m}[f_{mr}(t-t') + if_{mi}(t-t')], \tag{A3}$$

where,

$$f_{mr}(t) = \int_0^{\overline{\omega}} d\omega\, \omega \cos(\omega t)\coth\left(\frac{\hbar\omega}{2k_B T}\right), \tag{A4}$$

$$f_{mi}(t) = -\int_0^{\overline{\omega}} d\omega\, \omega \sin(\omega t). \tag{A5}$$

Here, T is the bath temperature, k_B is the Boltzmann constant, and $\overline{\omega}$ is the frequency cutoff of the reservoir spectrum. Note that the quantum Brownian motion of the mirror is non-Markovian in nature. Brownian noise is the thermal noise which arises due to the random motion of the movable mirror. The thermal noise term in the measured phase noise spectrum of the light reflected from the cavity is due to the quantum Brownian motion of the mirror [43]. Here the antisymmetric part, corresponding to f_{mi}, is a direct consequence of the commutation relation and it is never a Dirac delta while the symmetric part corresponding to f_{mr} explicitly depends on temperature and becomes proportional to a Dirac delta function only if the high-temperature limit $k_B T \gg \hbar\omega$ first and the infinite frequency cutoff limit $\omega \to \infty$ later are taken [52].

The quadratures $X_{in}(t)$ and $Y_{in}(t)$ satisfy the following correlations:

$$\langle X_{in}(t)X_{in}(t')\rangle = \langle Y_{in}(t)Y_{in}(t')\rangle = \delta(t-t'), \tag{A6}$$

$$\langle X_{in}(t)Y_{in}(t')\rangle = i\delta(t-t'), \tag{A7}$$

$$\langle Y_{in}(t)X_{in}(t')\rangle = -i\delta(t-t'). \tag{A8}$$

The generalized input noise, $a_{\eta'}(t)$, satisfies the following correlations [54]:

$$\langle a_{\eta'}(t)a_{\eta'}(t')\rangle = \langle a^{\dagger}_{\eta'}(t)a_{\eta'}(t')\rangle = 0, \tag{A9}$$

$$\langle a_{\eta'}(t)a^{\dagger}_{\eta'}(t')\rangle = \delta(t-t'), \tag{A10}$$

$$\langle a_{in}(t)a^{\dagger}_{\eta'}(t')\rangle = \langle a_{\eta'}(t)a^{\dagger}_{in}(t')\rangle = \sqrt{\eta'}\delta(t-t'). \tag{A11}$$

The corresponding generalized phase input noise is written as $Y^{\eta'}_{in}(t)$ which satisfies the following correlations:

$$\left\langle Y^{\eta'}_{in}(t)Y^{\eta'}_{in}(t')\right\rangle = \delta(t-t'), \tag{A12}$$

$$\left\langle X_{in}(t)Y^{\eta'}_{in}(t')\right\rangle = i\sqrt{\eta'}\delta(t-t'), \tag{A13}$$

$$\left\langle Y^{\eta'}_{in}(t)X_{in}(t')\right\rangle = -i\sqrt{\eta'}\delta(t-t'), \tag{A14}$$

$$\left\langle Y_{in}(t)Y^{\eta'}_{in}(t')\right\rangle = \sqrt{\eta'}\delta(t-t'), \tag{A15}$$

$$\left\langle Y^{\eta'}_{in}(t)Y_{in}(t')\right\rangle = \sqrt{\eta'}\delta(t-t'). \tag{A16}$$

APPENDIX B

The various coefficients of Sec. IV are as follows:

$$C_1(t) = \mathfrak{L}^{-1}\left[\frac{(s+\gamma_m)[s^2+AB]}{C(s)}\right], \tag{B1}$$

$$C_2(t) = \mathfrak{L}^{-1}\left[\frac{\omega_m[s^2+AB]}{C(s)}\right], \tag{B2}$$

$$C_3(t) = \mathfrak{L}^{-1}\left[\frac{-8g_{sc}g_c s(s+\gamma_m)}{C(s)}\right], \tag{B3}$$

$$C_4(t) = \mathfrak{L}^{-1}\left[\frac{-8g_{sc}g_c A(s+\gamma_m)}{C(s)}\right], \tag{B4}$$

$$C_5(t) = \mathfrak{L}^{-1}\left[\frac{4G\beta\omega_m[s^2+AB]+32Ag_{sc}g_c^2(s+\gamma_m)}{C(s)\sqrt{\gamma_c}}\right], \tag{B5}$$

$$C_6(t) = \mathfrak{L}^{-1}\left[\frac{s^2+AB}{C(s)}\right], \tag{B6}$$

$$C_7(t) = \mathfrak{L}^{-1}\left[\frac{(s-8G\beta g_{sc})(s^2+AB)}{C(s)}\right], \tag{B7}$$

$$C_8(t) = \mathfrak{L}^{-1}\left[\frac{8g_{sc}g_c\omega_m s}{C(s)}\right], \tag{B8}$$

$$C_9(t) = \mathfrak{L}^{-1}\left[\frac{8g_{sc}g_c A\omega_m}{C(s)}\right], \tag{B9}$$

$$C_{10}(t) = \mathfrak{L}^{-1}\left[\frac{[4G\beta(s^2+AB)](s-8G\beta g_{sc})-32A\omega_m g_{sc}g_c^2}{C(s)\sqrt{\gamma_c}}\right], \tag{B10}$$

$$C_{11}(t) = \mathfrak{L}^{-1}\left[\frac{-4Ag_c\omega_m^2-4Ag_c(s+\gamma_m)(s-8G\beta g_{sc})}{\sqrt{\gamma_c}C(s)}\right], \tag{B11}$$

$$C(s) = (s^2+AB)\left[\omega_m^2+(s+\gamma_m)(s-8G\beta g_{sc})\right], \tag{B12}$$

$$A = \nu + U_{\text{eff}}, \tag{B13}$$

$$B = \nu + 3U_{\text{eff}}. \tag{B14}$$

[1] C. M. Caves, Phys. Rev. Lett. **45**, 75 (1980).
[2] R. Loudon, Phys. Rev. Lett. **47**, 815 (1981).
[3] J. Mertz, O. Marti, and J. Mlynek, Appl. Phys. Lett. **62**, 2344 (1993).
[4] G. J. Milburn, K. Jacobs, and D. F. Walls, Phys. Rev. A **50**, 5256 (1994).
[5] T. W. Hansch and A. L. Schawlow, Opt. Commun. **13**, 68 (1975).
[6] D. J. Wineland, R. E. Drullinger, and F. L. Walls, Phys. Rev. Lett. **40**, 1639 (1978).
[7] S. Chu, L. Hollberg, J. E. Bjorkholm, A. Cable, and A. Ashkin, Phys. Rev. Lett. **55**, 48 (1985).
[8] T. Corbitt, Y. Chen, E. Innerhofer, H. Muller-Ebhardt, D. Ottaway, H. Rehbein, D. Sigg, S. Whitcomb, C. Wipf, and N. Mavalvala, Phys. Rev. Lett. **98**, 150802 (2007).
[9] C. Hohberger-Metzger and K. Karrai, Nature (London) **432**, 1002 (2004).
[10] S. Gigan *et al.*, Nature (London) **444**, 67 (2006).
[11] O. Arcizet *et al.*, Nature (London) **444**, 71 (2006).
[12] D. Kleckner and D. Bouwmeester, Nature (London) **444**, 75 (2006).
[13] I. Favero *et al.*, Appl. Phys. Lett. **90**, 104101 (2007).
[14] C. Regal, J. D. Terfel, and K. Lehnert, Nat. Phys. **4**, 555 (2008).
[15] T. Carmon, H. Rokhsari, L. Yang, T. J. Kippenberg, and K. J. Vahala, Phys. Rev. Lett. **94**, 223902 (2005).
[16] A. Schliesser, P. Del'Haye, N. Nooshi, K. J. Vahala, and T. J. Kippenberg, Phys. Rev. Lett. **97**, 243905 (2006).
[17] J. D. Thompson *et al.*, Nature (London) **452**, 72 (2008).
[18] C. Rossel *et al.*, Appl. Phys. **79**, 8166 (1996).
[19] J. K. Gimzewski, C. Gerber, E. Meyer, and R. R. Schlittler, Chem. Phys. Lett. **217**, 589 (1994).
[20] G. Binnig, C. F. Quate, and C. Gerber, Phys. Rev. Lett. **56**, 930 (1986).
[21] T. D. Stowe *et al.*, Appl. Phys. Lett. **71**, 14 (1997).
[22] D. Rugar, R. Budakian, H. J. Maim, and W. B. Chui, Nature (London) **430**, 329 (2004).
[23] Y. Hadjar, P.-F. Cohadon, C. G. Aminoff, M. Pinard, and A. Heidmann, Europhys. Lett. **47**, 545 (1999).
[24] B. Abbott *et al.*, Phys. Rev. Lett. **95**, 221101 (2005).
[25] G. M. Tino and F. Vetrano, Classical Quantum Gravity **24**, 2167 (2007).
[26] A. B. Bhattacherjee, Phys. Rev. A **80**, 043607 (2009).

[27] A. B. Bhattacherjee, J. Phys. B: At. Mol. Opt. Phys. **43**, 205301 (2010).
[28] F. Brennecke *et al.*, Science **322**, 235 (2008).
[29] K. W. Murch *et al.*, Nat. Phys. **4**, 561 (2008).
[30] P. Treutlein, D. Hunger, S. Camerer, T. W. Hansch, and J. Reichel, Phys. Rev. Lett. **99**, 140403 (2007).
[31] G. Szirmai, D. Nagy, and P. Domokos, Phys. Rev. A **81**, 043639 (2010).
[32] D. Hunger, S. Camerer, T. W. Hansch, D. Konig, J. P. Kotthaus, J. Reichel, and P. Treutlein, Phys. Rev. Lett. **104**, 143002 (2010).
[33] B. Chen, C. Jiang, and K. D. Zhu, Phys Rev. A **83**, 055803 (2011).
[34] G. De Chiara, M. Paternostro, and G. M. Palma, Phys. Rev. A **83**, 052324 (2011).
[35] S. K. Steinke and P. Meystre, Phys. Rev. A **84**, 023834 (2011).
[36] D. Hunger *et al.*, C. R. Phys. **12**, 871 (2011).
[37] B. Chen *et al.*, J. Opt. Soc. Am. **28**, 2007 (2011).
[38] K. Zhang, W. Chen, M. Bhattacharya, and P. Meystre, Phys. Rev. A **81**, 013802 (2010).
[39] B. Nagorny, Th. Elsasser, and A. Hemmerich, Phys. Rev. Lett. **91**, 153003 (2003).
[40] J. A. Sauer, K. M. Fortier, M. S. Chang, C. D. Hamley, and M. S. Chapman, Phys. Rev. A **69**, 051804 (2004).
[41] A. Ottl, S. Ritter, M. Kohl, and T. Esslinger, Phys. Rev. Lett. **95**, 090404 (2005).
[42] I. Tittonen, G. Breitenbach, T. Kalkbrenner, T. Muller, R. Conradt, S. Schiller, E. Steinsland, N. Blanc, and N. F. de Rooij, Phys. Rev. A **59**, 1038 (1999).
[43] S. Mancini, D. Vitali, and P. Tombesi, Phys. Rev. Lett. **80**, 688 (1998); D. Vitali, S. Mancini, L. Ribichini, and P. Tombesi, Phys. Rev. A. **65**, 063803 (2002).
[44] S. van der Meer, Rev. Mod. Phys. **57**, 689 (1985).
[45] C. L. Degan, M. Poggio, H. J. Mamin, and D. Rugar, Phys. Rev. Lett. **99**, 250601 (2007).
[46] O. Arcizet, P. F. Cohadon, T. Briant, M. Pinard, A. Heidmann, J. M. Mackowski, C. Michel, L. Pinard, O. Francais, and L. Rousseau, Phys. Rev. Lett. **97**, 133601 (2006).
[47] H. P. Yuen, Phys. Rev. Lett. **51**, 719 (1983).
[48] M. Paternostro, G. De Chiara, and G. M. Palma, Phys. Rev. Lett. **104**, 243602 (2010).
[49] A. N. Cleland and M. L. Roukes, Nature (London) **392**, 160 (1998).
[50] S. Camerer, M. Korppi, A. Jöckel, D. Hunger, T. W. Hänsch, and P. Treutlein, Phys. Rev. Lett. **107**, 223001 (2011).
[51] M. Pinard, Y. Hadjar, and A. Heidmann, Eur. Phys. J. D **7**, 107 (1999).
[52] V. Giovannetti and D. Vitali, Phys. Rev. A **63**, 023812 (2001).
[53] V. B. Braginski and F. Y. Khalilli, *Quantum Measurements* (Cambridge University Press, Cambridge, 1992).
[54] V. Giovannetti, P. Tombesi, and D. Vitali, Phys. Rev. A **60**, 1549 (1999).
[55] B. Nagorny, T. Elsasser, H. Richter, A. Hemmerich, D. Kruse, C. Zimmermann, and P. Courteille, Phys. Rev. A **67**, 031401(R) (2003).
[56] M. Theis, G. Thalhammer, K. Winkler, M. Hellwig, G. Ruff, R. Grimm, and J. H. Denschlag, Phys. Rev. Lett. **93**, 123001 (2004).
[57] Garrett D. Cole, Proc. SPIE **8458**, 845807 (2012).
[58] A. Schliesser *et al.*, Nat. Phys. **4**, 415 (2008).
[59] P. F. Cohadon, A. Heidmann, and M. Pinard, Phys. Rev. Lett. **83**, 3174 (1999).
[60] M. Pinard, P. F. Cohadon, T. Briant, and A. Heidmann, Phys. Rev. A **63**, 013808 (2000).